Journal of King Saud University – Science 33 (2021) 101643

Contents lists available at ScienceDirect

Journal of King Saud University – Science

journal homepage: www.sciencedirect.com

Original article

Construction of new exact solutions of the resonant fractional NLS equation with the extended Fan sub-equation method

Kalim U. Tariq [a], Eric Tala-Tebue [b], Hadi Rezazadeh [c], Muhammad Younis [d], Ahmet Bekir [e], Yu-Ming Chu [f,g,*]

[a] Department of Mathematics, Mirpur University of Science and Technology, Mirpur 10250, AJK, Pakistan
[b] Laboratoire d'Automatique et d'Informatique Appliquee (LAIA), IUT-FV of Bandjoun, The University of Dschang, Bandjoun BP 134, Cameroon
[c] Faculty of Engineering Technology, Amol University of Special Modern Technological, Amol, Iran
[d] Centre for Undergraduate Studies, University of the Punjab, Lahore 54590, Pakistan
[e] Neighbourhood of Akcaglan, Imarli Street, 28/4, Eskisehir 26030, Turkey
[f] Department of Mathematics, Huzhou University, Huzhou 313000, PR China
[g] Hunan Provincial Key Laboratory of Mathematical Modeling and Analysis in Engineering, Changsha University of Science and Technology, Changsha 410114, PR China

A R T I C L E I N F O

Article history:
Received 28 November 2020
Revised 23 September 2021
Accepted 1 October 2021
Available online 13 October 2021

Keywords:
Resonant fractional nonlinear Schrödinger equation
Extended Fan sub-equation method
New solutions

A B S T R A C T

The fucus of this study is to find a set of some novel solutions concerning the resonant fractional nonlinear Schrödinger equation (R-FNLSE) with quadratic-cubic nonlinearity by employing the extended FAN sub-equation approach. The parameter $\alpha \in (0, 1]$ is the core constraint which simulate the flow rate propagation, plays a key rote in telecommunications and the theory of optical fibres. This equation expresses the gesture of solitons and Madelung fluids in various nonlinear systems. These outcomes are optical, bright, dark, explicit, periodic and combined wave solutions and efficiently demonstrated with the aid of 3D plots. The representation of these solutions is carried out in order to have an idea about the structure of such model and can also be extended to many other complex models of recent era.

1. Introduction

In recent decades, it has been noticed that nonlinear phenomena have remarkable properties in physics and mathematical engineering. The phenomenon of nonlinear evaluation equations (NLEE) has received a lot of attention and has become one of the most interesting areas of research. Such type of models are widely used to elucidate many complex physical phenomena that occur in fluid and plasma wave mechanics, fiber optic communications, biophysics, Soliton's theory, and many more (Kalim et al., 2018; Ghanbari et al., 2019a; Ghanbari et al., 2019b; Munusamy et al., 2020; Rezazadeh, 2018).

The area of nonlinear partial differential equations is becoming one of the most essential disciplines describing dynamics of key phenomena of nature and has attracted renowned researchers and scientists in the theory of optical fibre arising in telecommunications, spectroscopy, plasma physics and many more. Optical solitons are basically localized electromagnetic waves which can transmit large amount of information through optical fibers across the trans-oceanic distance in femto-seconds. In the modern era of science and technology, the theory of solitons has created revolutionary developments in the telecommunication engineering and is one of the most blistering field of research over the past few decades and reckon as the technology of future generation for high-speed communication systems (Ghanbari et al., 2020; Hosseini et al., 2020a; Hosseini et al., 2020b; Korpinar et al., 2019; Hashemi et al., 2019).

Many complex phenomena in diverse areas of nonlinear science are usually described by nonlinear models. One of the most famous of these nonlinear equations is the Schrödinger's equation. This equation has been used in several domains among which: fiber optics, hydrodynamics, Plasma physics, nonlinear electrical transmission lines, and so on (Liu et al., 2019). However, there are a multitude of nonlinear equations such as the Ginzburg–Landau equation (Wazwaz, 2006), the Korteweg de Vries equation (Seadawy et al., 2020), the Zoomeron equation (Hosseini et al., 2020c), the Boussinesq equation (Mehdinejadiani and Parviz, 2020), to mention a few, that can also help to describe many sys-

* Corresponding author at: Department of Mathematics, Huzhou University, Huzhou 313000, PR China.
E-mail address: chuyuming@zjhu.edu.cn (Y.-M. Chu).

Peer review under responsibility of King Saud University.

Production and hosting by Elsevier

https://doi.org/10.1016/j.jksus.2021.101643
1018-3647/

tems. It's worth mentioning that integer order derivatives are previously utilised to analyze these problems. However, in order to gain a better understanding of the dynamics of these nonlinear equations, a common type of derivative called fractional derivatives should be presented (Manafian and Lakestani, 2017; Miller and Ross, 1993).

This concept is a generalization of derivatives. Thus, we observe that the fractional NLEE is a natural extension of a NLEE of integeral order. These fractional differential equations are generally not easy to solve and methods that have been proposed in the literature to transform them are used. Among these methods, we can list the Caputo fractional derivatives, the Riemann–Liouville fractional derivatives, modified Riemann–Liouville derivative, conformable fractional derivative. The enactment of such methods is just a beginning for a revolution of recent era towards fractional calculus. To date, there are several methods in the literature that can be implemented to deal with the nonlinear models arising in diverse disciplines (Goswami et al., 2020; Singh et al., 2021a; Singh et al., 2021b; Singh et al., 2021c).

The outline of this study is given as follows: in Section 2, a brief introduction to the R-FNLSE with quadratic-cubic nonlinearity is illustrated whereas in Section 3 some noval anlytical solutions to the nonlinear complex model (1) are established. The geometrical behavior of the solutions is demonstrated in Section 4. At the end, the conclusions have been extracted.

2. The R-FNLSE with quadratic-cubic nonlinearity

Over the last few decades, the study solitonic and optical behaviour of nonlinear models is becoming one of the most excited topics in the diverse disciplines of contemporary science. Our prospective is applicable until the given model imply more even odd order partial derivative terms (Seadawy and Lu, 2017; Younis et al., 2020).

Over the last couple of years, many computational analysis have been established effectively to describe the soliton solutions of various type of nonlinear Schrödinger equation (NLSE) among these are, the extended sinh-Gordon equation expansion method (Baskonus et al., 2018), extended Jocobi's elliptic approach (Hong and Lu, 2009), the modified auxiliary equation mapping method (Seadawy et al., 2020), the inverse scattering transformation method (Zhang and Chen, 2019), extended rational sine–cosine method (Mahak and Akram, 2019), and many more.

The purpose of the study is to investigate the NLSE of fractional order (Bhrawy et al., 2014) with quadratic-cubic nonlinearity, as well as perturbation terms and higher order dispersions (third and fourth order dispersions). The R-FNLSE with quadratic-cubic nonlinearity is studied by using extended Fan sub-equation (EFSE) approach.

$$\begin{aligned} & i\{\delta\Phi_x - \gamma\Phi_{xxx} - i\sigma\Phi_{xxxx} + \varrho(|\Phi|^2\Phi)_x + \theta(|\Phi|^2)_x\Phi\} \\ & \quad + iD^\alpha\Phi + \varsigma_1\Phi_{xx} + (\varsigma_2(|\Phi|) + \varsigma_3\left(|\Phi|^2\right))\Phi = 0, \end{aligned} \tag{1}$$

where D^α is the conformable derivative operator of order $\alpha \in (0,1]$ in t-direction and the parameters $\varsigma_j (j = 1,2,3)$ are the coefficients of group velocity dispersion, quadratic and cubic nonlinearity respectively, for details see (Triki et al., 2017; Eslami et al., 2013).

3. Applications to the EFSE method

The transformation

$$\Phi(x,t) = \Omega(\xi)e^{i\psi}, \tag{2}$$

where

$$\xi = x - \left(\frac{\nu}{\alpha}\right)t^\alpha, \quad \psi = \theta - \kappa x + \left(\frac{\omega}{\alpha}\right)t^\alpha, \tag{3}$$

κ, σ and θ are the frequency, the wave number and the phase constant respectively, reduces Eq. (1) into real and imaginary factors

$$-\Omega\left(\Omega^2(\varsigma_3 - \kappa\varrho) + \varsigma_2\Omega\right) - \gamma_2\Omega'' + \gamma_1\Omega + \sigma\Omega'''' = 0, \tag{4}$$

where

$$\gamma_1 = \varsigma_1\kappa^2 + \gamma\kappa^3 + \delta\kappa + \kappa^4\sigma + \omega, \gamma_2 = \varsigma_1 + \gamma\kappa + 6\kappa^3\sigma,$$

and

$$(\nu + 2\varsigma_1\kappa + \delta + 3\gamma\kappa^2 + 4\sigma\kappa^3)\Omega' - (\gamma + 4\sigma\kappa)\Omega'' + (3\varrho + 2\theta)\Omega^2\Omega' = 0, \tag{5}$$

gives

$$\nu = -2\varsigma_1\kappa - \delta - 3\gamma\kappa^2 - 4\sigma\kappa^4, \gamma + 4\sigma\kappa = 0, 3\varrho + 2\theta = 0.$$

The solution for Eq. (4) is of the fashion (Kalim et al., 2021; El-Wakil and Abdou, 2008)

$$\Omega = \mathfrak{a}_0 + \mathfrak{a}_1\phi(\xi) + \mathfrak{a}_2\phi^2(\xi), \tag{6}$$

such that

$$\left(\frac{d\phi(\xi)}{d\xi}\right)^2 = \ell_0 + \ell_1\phi(\xi) + \ell_2\phi^2(\xi) + \ell_3\phi^3(\xi) + \ell_4\phi^4(\xi), \tag{7}$$

$\ell_i (i = 0,1,2,3,4)$ are real constants.

Inserting Eq. (6) along Eq. (7) in Eq. (4) and picking the coefficients of $\phi^j\phi^{(k)}$,

$$\begin{aligned} & \mathfrak{a}_0\gamma_1 + \mathfrak{a}_0^3(-(\varsigma_3 - \kappa\varrho)) - \mathfrak{a}_0^2\varsigma_2 - 2\mathfrak{a}_2\gamma_2\ell_0 - \tfrac{1}{2}\mathfrak{a}_1\gamma_2\ell_1 \\ & + \tfrac{3}{2}\mathfrak{a}_2\ell_1^2\sigma + 8\mathfrak{a}_2\ell_0\ell_2\sigma + \tfrac{1}{2}\mathfrak{a}_1\ell_1\ell_2\sigma + 3\mathfrak{a}_1\ell_0\ell_3\sigma = 0, \\ & \mathfrak{a}_1\gamma_1 - 3\mathfrak{a}_1\mathfrak{a}_0^2(\varsigma_3 - \kappa\varrho) - 2\mathfrak{a}_1\mathfrak{a}_0\varsigma_2 - 3\mathfrak{a}_2\gamma_2\ell_1 - \mathfrak{a}_1\gamma_2\ell_2 \\ & + \mathfrak{a}_1\ell_2^2\sigma + 15\mathfrak{a}_2\ell_1\ell_2\sigma + 30\mathfrak{a}_2\ell_0\ell_3\sigma + \tfrac{9}{2}\mathfrak{a}_1\ell_1\ell_3\sigma + 12\mathfrak{a}_1\ell_0\ell_4\sigma = 0, \\ & \mathfrak{a}_2\gamma_1 - 3\mathfrak{a}_2\mathfrak{a}_0^2(\varsigma_3 - \kappa\varrho) - 3\mathfrak{a}_1^2\mathfrak{a}_0(\varsigma_3 - \kappa\varrho) - 2\mathfrak{a}_2\mathfrak{a}_0\varsigma_2 \\ & - \mathfrak{a}_1^2\varsigma_2 - 4\mathfrak{a}_2\gamma_2\ell_2 - \tfrac{3}{2}\mathfrak{a}_1\gamma_2\ell_3 + 16\mathfrak{a}_2\ell_2^2\sigma + 42\mathfrak{a}_2\ell_1\ell_3\sigma \\ & + \tfrac{15}{2}\mathfrak{a}_1\ell_2\ell_3\sigma + 72\mathfrak{a}_2\ell_0\ell_4\sigma + 15\mathfrak{a}_1\ell_1\ell_4\sigma = 0, \\ & a_1^3(-(\varsigma_3 - \kappa\varrho)) - 6\mathfrak{a}_0\mathfrak{a}_2\mathfrak{a}_1(\varsigma_3 - \kappa\varrho) - 2\mathfrak{a}_2\mathfrak{a}_1\varsigma_2 - 2\mathfrak{a}_1\gamma_2\ell_4 \\ & - 5a_2\gamma_2\ell_3 + \tfrac{15}{2}\mathfrak{a}_1\ell_3^2\sigma + 20\mathfrak{a}_1\ell_2\ell_4\sigma + 65\mathfrak{a}_2\ell_2\ell_3\sigma + 90\mathfrak{a}_2\ell_1\ell_4\sigma = 0, \\ & -3\mathfrak{a}_2\mathfrak{a}_1^2(\varsigma_3 - \kappa\varrho) - 3\mathfrak{a}_0\mathfrak{a}_2^2(\varsigma_3 - \kappa\varrho) - \mathfrak{a}_2^2\ell_2 - 6\mathfrak{a}_2\gamma_2\ell_4 \\ & + 30\mathfrak{a}_1\ell_3\ell_4\sigma + \tfrac{105}{2}\mathfrak{a}_2\ell_3^2\sigma + 120\mathfrak{a}_2\ell_2\ell_4\sigma = 0, \\ & -3\mathfrak{a}_1\mathfrak{a}_2^2(\varsigma_3 - \kappa\varrho) + 168\mathfrak{a}_2\ell_3\ell_4\sigma + 24\mathfrak{a}_1\ell_4^2\sigma = 0, \\ & 120\mathfrak{a}_2\ell_4^2\sigma - \mathfrak{a}_2^3(\varsigma_3 - \kappa\varrho) = 0. \end{aligned}$$

We select variables suitably which gives

$$\mathfrak{a}_0 = \frac{4\ell_4\left(\sqrt{30}\varsigma_2\sqrt{\sigma} + 3\sqrt{\varsigma_3 - \kappa\varrho}(20\ell_2\sigma - \gamma_2)\right) - 45\ell_3^2\sigma\sqrt{\varsigma_3 - \kappa\varrho}}{12\sqrt{30}\ell_4\sqrt{\sigma}(\kappa\varrho - \varsigma_3)}, \tag{8}$$

$$\mathfrak{a}_1 = \frac{\sqrt{30}\ell_3\sqrt{\sigma}}{\sqrt{\varsigma_3 - \kappa\varrho}}, \tag{9}$$

$$\mathfrak{a}_2 = \frac{2\sqrt{30}\ell_4\sqrt{\sigma}}{\sqrt{\varsigma_3 - \kappa\varrho}}. \tag{10}$$

We have soliton solutions

$$\Phi(x,t) = \left(\mathfrak{a}_0 + \mathfrak{a}_1\phi(\xi) + \mathfrak{a}_2\phi^2(\xi)\right)e^{i\psi}. \tag{11}$$

Case I

If $\ell_0 = \vartheta_3^2, \ell_1 = 2\vartheta_1\vartheta_3, \ell_2 = 2\vartheta_2\vartheta_3 + \vartheta_1^2, \ell_3 = 2\vartheta_1\vartheta_2, \ell_4 = \vartheta_2^2$, there may exist parameters ϑ_1, ϑ_2, satisfy ϑ_3, the solutions of (1) are $\phi_\eta^I, (\eta = 1,2,\ldots,24)$.

Type I.

$\vartheta_1^2-4\vartheta_2\vartheta_3>0,\ \vartheta_1\vartheta_2\neq 0,\ \vartheta_2\vartheta_3\neq 0$. We obtain the dark optical solitons in the form as follows

$$\phi_1^I(x,t)=\left[\mathfrak{a}_0+\mathfrak{a}_1\left(-\frac{\sqrt{\vartheta_1^2-4\vartheta_2\vartheta_3}\tanh\left(\frac{1}{2}\xi\sqrt{\vartheta_1^2-4\vartheta_2\vartheta_3}\right)+\vartheta_1}{2\vartheta_2}\right)+\mathfrak{a}_2\left(-\frac{\sqrt{\vartheta_1^2-4\vartheta_2\vartheta_3}\tanh\left(\frac{1}{2}\xi\sqrt{\vartheta_1^2-4\vartheta_2\vartheta_3}\right)+\vartheta_1}{2\vartheta_2}\right)^2\right]\times e^{i\psi}. \tag{12}$$

We obtain the combined bright-dark optical soliton in the form as follows

$$\begin{aligned}\phi_3^I(x,t)=&\left[\mathfrak{a}_0-\frac{\mathfrak{a}_1}{2\vartheta_2}\left(\sqrt{\vartheta_1^2-4\vartheta_2\vartheta_3}\left(i\operatorname{sech}\left(\xi\sqrt{\vartheta_1^2-4\vartheta_2\vartheta_3}\right)\right.\right.\right.\\&\left.\left.+\tanh\left(\xi\sqrt{\vartheta_1^2-4\vartheta_2\vartheta_3}\right)\right)+\vartheta_1\right)\\&+\frac{\mathfrak{a}_2}{2\vartheta_2}\left(\sqrt{\vartheta_1^2-4\vartheta_2\vartheta_3}\left(i\operatorname{sech}\left(\xi\sqrt{\vartheta_1^2-4\vartheta_2\vartheta_3}\right)\right.\right.\\&\left.\left.\left.+\tanh\left(\xi\sqrt{\vartheta_1^2-4\vartheta_2\vartheta_3}\right)\right)+\vartheta_1\right)^2\right]\times e^{i\psi}.\end{aligned} \tag{13}$$

We obtain the combined dark-singular optical solitons in the form as follows

$$\begin{aligned}\phi_5^I(x,t)=&\left[\mathfrak{a}_0-\frac{\mathfrak{a}_1}{2\vartheta_2}\left(\sqrt{\vartheta_1^2-4\vartheta_2\vartheta_3}\left(\tanh\left(\frac{1}{4}\xi\sqrt{\vartheta_1^2-4\vartheta_2\vartheta_3}\right)\right.\right.\right.\\&\left.\left.+\coth\left(\frac{1}{4}\xi\sqrt{\vartheta_1^2-4\vartheta_2\vartheta_3}\right)\right)+\vartheta_1\right)\\&+\frac{\mathfrak{a}_2}{2\vartheta_2}\left(\sqrt{\vartheta_1^2-4\vartheta_2\vartheta_3}\left(\tanh\left(\frac{1}{4}\xi\sqrt{\vartheta_1^2-4\vartheta_2\vartheta_3}\right)\right.\right.\\&\left.\left.\left.+\coth\left(\frac{1}{4}\xi\sqrt{\vartheta_1^2-4\vartheta_2\vartheta_3}\right)\right)+\vartheta_1\right)^2\right]\times e^{i\psi}.\end{aligned} \tag{14}$$

$$\begin{aligned}\phi_{10}^I(x,t)=&\left[\mathfrak{a}_0+\mathfrak{a}_1\left(\left(2\cosh\left(\xi\sqrt{\vartheta_1^2-4\vartheta_2\vartheta_3}\right)\right)\left(\sqrt{\vartheta_1^2-4\vartheta_2\vartheta_3}\right.\right.\right.\\&\sinh\left(\xi\sqrt{\vartheta_1^2-4\vartheta_2\vartheta_3}\right)-\left(\vartheta_1\cosh\left(\xi\sqrt{\vartheta_1^2-4\vartheta_2\vartheta_3}\right)\right.\\&\left.\left.\left.\pm i\sqrt{\vartheta_1^2-4\vartheta_2\vartheta_3}\right)\right)^{-1}\right)\\&+\mathfrak{a}_2\left(\left(\left(2\cosh\left(\xi\sqrt{\vartheta_1^2-4\vartheta_2\vartheta_3}\right)\right)\left(\sqrt{\vartheta_1^2-4\vartheta_2\vartheta_3}\right.\right.\right.\\&\sinh\left(\xi\sqrt{\vartheta_1^2-4\vartheta_2\vartheta_3}\right)-\left(\vartheta_1\cosh\left(\xi\sqrt{\vartheta_1^2-4\vartheta_2\vartheta_3}\right)\right.\\&\left.\left.\left.\left.\pm i\sqrt{\vartheta_1^2-4\vartheta_2\vartheta_3}\right)\right)^{-1}\right)^2\right]\times e^{i\psi}.\end{aligned} \tag{15}$$

Type II.

$\vartheta_1^2-4\vartheta_2\vartheta_3<0,\ \vartheta_1\vartheta_2\neq 0,\ \vartheta_2\vartheta_3\neq 0$. The collection of periodic solitons are obtained

$$\phi_{13}^I(x,t)=\left[\mathfrak{a}_0+\mathfrak{a}_1\left(-\frac{\sqrt{4\vartheta_2\vartheta_3-\vartheta_1^2}\tan\left(\frac{1}{2}\xi\sqrt{4\vartheta_2\vartheta_3-\vartheta_1^2}\right)-\vartheta_1}{2\vartheta_2}\right)+\mathfrak{a}_2\left(-\frac{\sqrt{4\vartheta_2\vartheta_3-\vartheta_1^2}\tan\left(\frac{1}{2}\xi\sqrt{4\vartheta_2\vartheta_3-\vartheta_1^2}\right)-\vartheta_1}{2\vartheta_2}\right)^2\right]\times e^{i\psi}, \tag{16}$$

$$\begin{aligned}\phi_{20}^I(x,t)=&\left[\mathfrak{a}_0+\mathfrak{a}_1\left(-\frac{2\vartheta_3\cos\left(\frac{1}{2}\xi\sqrt{4\vartheta_2\vartheta_3-\vartheta_1^2}\right)}{\sqrt{4\vartheta_2\vartheta_3-\vartheta_1^2}\sin\left(\frac{1}{2}\xi\sqrt{4\vartheta_2\vartheta_3-\vartheta_1^2}\right)+\vartheta_1\cos\left(\frac{1}{2}\xi\sqrt{4\vartheta_2\vartheta_3-\vartheta_1^2}\right)}\right)\right.\\&\left.+\mathfrak{a}_2\left(-\frac{2\vartheta_3\cos\left(\frac{1}{2}\xi\sqrt{4\vartheta_2\vartheta_3-\vartheta_1^2}\right)}{\sqrt{4\vartheta_2\vartheta_3-\vartheta_1^2}\sin\left(\frac{1}{2}\xi\sqrt{4\vartheta_2\vartheta_3-\vartheta_1^2}\right)+\vartheta_1\cos\left(\frac{1}{2}\xi\sqrt{4\vartheta_2\vartheta_3-\vartheta_1^2}\right)}\right)^2\right]\times e^{i\psi},\end{aligned} \tag{17}$$

$$\begin{aligned}\phi_{24}^I(x,t)=&\left[\mathfrak{a}_0+\mathfrak{a}_1\left(\left(4r\sin\left(\frac{1}{4}\xi\sqrt{4\vartheta_2\vartheta_3-\vartheta_1^2}\right)\cos\left(\frac{1}{4}\xi\sqrt{4\vartheta_2\vartheta_3-\vartheta_1^2}\right)\right)\right.\right.\\&\left(2\sqrt{4\vartheta_2\vartheta_3-\vartheta_1^2}\cos^2\left(\frac{1}{4}\xi\sqrt{4\vartheta_2\vartheta_3-\vartheta_1^2}\right)-2\vartheta_1\sin\left(\frac{1}{4}\xi\sqrt{4\vartheta_2\vartheta_3-\vartheta_1^2}\right)\right.\\&\left.\left.\cos\left(\frac{1}{4}\xi\sqrt{4\vartheta_2\vartheta_3-\vartheta_1^2}\right)-\sqrt{4\vartheta_2\vartheta_3-\vartheta_1^2}\right)^{-1}\right)\\&+\mathfrak{a}_2\left(\left(\left(4r\sin\left(\frac{1}{4}\xi\sqrt{4\vartheta_2\vartheta_3-\vartheta_1^2}\right)\cos\left(\frac{1}{4}\xi\sqrt{4\vartheta_2\vartheta_3-\vartheta_1^2}\right)\right)\right.\right.\\&\left(2\sqrt{4\vartheta_2\vartheta_3-\vartheta_1^2}\cos^2\left(\frac{1}{4}\xi\sqrt{4\vartheta_2\vartheta_3-\vartheta_1^2}\right)-2\vartheta_1\sin\left(\frac{1}{4}\xi\sqrt{4\vartheta_2\vartheta_3-\vartheta_1^2}\right)\right.\\&\left.\left.\left.\cos\left(\frac{1}{4}\xi\sqrt{4\vartheta_2\vartheta_3-\vartheta_1^2}\right)-\sqrt{4\vartheta_2\vartheta_3-\vartheta_1^2}\right)^{-1}\right)^2\right]\times e^{i\psi}.\end{aligned} \tag{18}$$

Case II

If $\ell_0=\vartheta_3^2,\ell_1=2\vartheta_1\vartheta_3,\ell_2=0,\ell_3=2\vartheta_1\vartheta_2,\ell_4=\vartheta_2^2,\phi$ is one of the $\phi_\eta^{II},(\eta=1,2,\dots,12)$. A collection of dark optical soliton is observed

$$\phi_1^{II}(x,t)=\left[\mathfrak{a}_0+\mathfrak{a}_1\left(-\frac{\sqrt{-6\vartheta_2\vartheta_3}\tanh\left(\frac{1}{2}\xi\sqrt{-6\vartheta_2\vartheta_3}\right)+\sqrt{-2\vartheta_2\vartheta_3}}{2\vartheta_2}\right)+\mathfrak{a}_2\left(-\frac{\sqrt{-6\vartheta_2\vartheta_3}\tanh\left(\frac{1}{2}\xi\sqrt{-6\vartheta_2\vartheta_3}\right)+\sqrt{-2\vartheta_2\vartheta_3}}{2\vartheta_2}\right)^2\right]\times e^{i\psi}. \tag{19}$$

$$\begin{aligned}\phi_5^{II}(x,t)=&\left[\mathfrak{a}_0-\frac{\mathfrak{a}_1}{4\vartheta_2}\left(\sqrt{-6\vartheta_2\vartheta_3}\left(\tanh\left(\frac{1}{4}\xi\sqrt{-6\vartheta_2\vartheta_3}\right)\right.\right.\right.\\&\left.\left.+\coth\left(\frac{1}{4}\xi\sqrt{-6\vartheta_2\vartheta_3}\right)\right)+2\sqrt{-2\vartheta_2\vartheta_3}\right)\\&+\frac{\mathfrak{a}_2}{4\vartheta_2}\left(\sqrt{-6\vartheta_2\vartheta_3}\left(\tanh\left(\frac{1}{4}\xi\sqrt{-6\vartheta_2\vartheta_3}\right)\right.\right.\\&\left.\left.\left.+\coth\left(\frac{1}{4}\xi\sqrt{-6\vartheta_2\vartheta_3}\right)\right)+2\sqrt{-2\vartheta_2\vartheta_3}\right)^2\right]\times e^{i\psi}.\end{aligned} \tag{20}$$

Case III

$\ell_0=\ell_1=0$, we have the following solution of (1) in the form $\phi_\eta^{III},(\eta=1,2,\dots,10)$.

Type I.

$\ell_2=1,\ell_3=\frac{-2\varrho_3}{\varrho_1},\ell_4=\frac{\varrho_3^2-\varrho_2^2}{\varrho_1^2}$, where $\varrho_1,\varrho_2,\varrho_3$ are arbitrary constants.

$$\phi_1^{III}(x,t)=\left[\mathfrak{a}_0+\mathfrak{a}_1\left(\frac{\varrho_1\operatorname{sech}(\xi)}{\varrho_2\operatorname{sech}(\xi)+\varrho_3}\right)+\mathfrak{a}_2\left(\frac{\varrho_1\operatorname{sech}(\xi)}{\varrho_2\operatorname{sech}(\xi)+\varrho_3}\right)^2\right]\times e^{i\psi}. \tag{21}$$

Type II

$\ell_2=1,\ell_3=\frac{-2\varrho_3}{\varrho_1},\ell_4=\frac{\varrho_3^2+\varrho_2^2}{\varrho_1^2}$, where $\varrho_1,\varrho_2,\varrho_3$ are arbitrary constants.

$$\phi_2^{III}(x,t)=\left[\mathfrak{a}_0+\mathfrak{a}_1\left(\frac{\varrho_1\operatorname{csch}(\xi)}{\varrho_2\operatorname{csch}(\xi)+\varrho_3}\right)+\mathfrak{a}_2\left(\frac{\varrho_1\operatorname{csch}(\xi)}{\varrho_2\operatorname{csch}(\xi)+\varrho_3}\right)^2\right]\times e^{i\psi}. \tag{22}$$

Eqs. (21), (22) give a set of bright and singular optical solitons for $\varrho_2=0$

$$\phi_1^{III}(x,t)=\left[\mathfrak{a}_0+\mathfrak{a}_1\left(\frac{\varrho_1\operatorname{sech}(\xi)}{\varrho_3}\right)+\mathfrak{a}_2\left(\frac{\varrho_1\operatorname{sech}(\xi)}{\varrho_3}\right)^2\right]\times e^{i\psi}. \tag{23}$$

$$\phi_2^{III}(x,t)=\left[\mathfrak{a}_0+\mathfrak{a}_1\left(\frac{\varrho_1\operatorname{csch}(\xi)}{\varrho_3}\right)+\mathfrak{a}_2\left(\frac{\varrho_1\operatorname{csch}(\xi)}{\varrho_3}\right)^2\right]\times e^{i\psi}. \tag{24}$$

Type III

$\ell_2=4,\ell_3=-\frac{4(2\varrho_2+\varrho_4)}{\varrho_1},\ell_4=\frac{4\varrho_2^2+4\varrho_4\varrho_2+\varrho_3^2}{\varrho_1^2}$, where $\varrho_1,\varrho_2,\varrho_3,\varrho_4$ are arbitrary constants.

$$\phi_3^{III}(x,t)=\left[\mathfrak{a}_0+\mathfrak{a}_1\left(\frac{\varrho_1\operatorname{sech}^2(\xi)}{\varrho_2\tanh(\xi)+\varrho_3+\varrho_4\operatorname{sech}^2(\xi)}\right)+\mathfrak{a}_2\left(\frac{\varrho_1\operatorname{sech}^2(\xi)}{\varrho_2\tanh(\xi)+\varrho_3+\varrho_4\operatorname{sech}^2(\xi)}\right)^2\right]\times e^{i\psi}. \tag{25}$$

Type IV

$\ell_2 = 4, \ell_3 = \frac{4(\varrho_4 - 2\varrho_2)}{\varrho_1}, \ell_4 = \frac{4\varrho_2^2 - 4\varrho_4\varrho_2 + \varrho_3^2}{\varrho_1^2}$, where $\varrho_1, \varrho_2, \varrho_3, \varrho_4$ are arbitrary constants.

$$\phi_4^{III}(x,t) = \left[\alpha_0 + \alpha_1\left(\frac{\varrho_1 \operatorname{csch}^2(\xi)}{\varrho_2\coth(\xi) + \varrho_3 + \varrho_4\operatorname{csch}^2(\xi)}\right) + \alpha_2\left(\frac{\varrho_1 \operatorname{csch}^2(\xi)}{\varrho_2\coth(\xi) + \varrho_3 + \varrho_4\operatorname{csch}^2(\xi)}\right)^2\right] \times e^{i\psi}. \tag{26}$$

Another class of dark and singular optical solitons is obtained for $\varrho_2 = \varrho_4$

$$\phi_4^{III}(x,t) = \left[\alpha_0 + \alpha_1\left(\frac{\varrho_1 \operatorname{csch}^2(\xi)}{\varrho_2\coth(\xi) + \varrho_3 + \varrho_2\operatorname{csch}^2(\xi)}\right) + \alpha_2\left(\frac{\varrho_1 \operatorname{csch}^2(\xi)}{\varrho_2\coth(\xi) + \varrho_3 + \varrho_2\operatorname{csch}^2(\xi)}\right)^2\right] \times e^{i\psi}. \tag{27}$$

Type V

$\ell_2 = -1, \ell_3 = \frac{2\varrho_3}{\varrho_1}, \ell_4 = \frac{\varrho_3^2 - \varrho_2^2}{\varrho_1^2}$, where $\varrho_1, \varrho_2, \varrho_3$ are arbitrary constants.

$$\phi_6^{III}(x,t) = \left[\alpha_0 + \alpha_1\left(-\frac{\varrho_1(\sinh(\varrho_1\xi) + \cosh(\varrho_1\xi))(\sinh(\varrho_1\xi) + \cosh(\varrho_1\xi) + \varrho_2)}{\varrho_3}\right) + \alpha_2\left(-\frac{\varrho_1(\sinh(\varrho_1\xi) + \cosh(\varrho_1\xi))(\sinh(\varrho_1\xi) + \cosh(\varrho_1\xi) + \varrho_2)}{\varrho_3}\right)^2\right] \times e^{i\psi}. \tag{28}$$

Type VI

$\ell_2 = 4, \ell_3 = \frac{-2\varrho_3}{\varrho_1}, \ell_4 = \frac{\varrho_3^2 - \varrho_2^2}{\varrho_1^2}$, where $\varrho_1, \varrho_2, \varrho_3$ are arbitrary constants.

$$\phi_8^{III}(x,t) = \left[\alpha_0 + \alpha_1\left(\frac{\varrho_1\csc(\xi)}{\varrho_2\csc(\xi) + \varrho_3}\right) + \alpha_2\left(\frac{\varrho_1\csc(\xi)}{\varrho_2\csc(\xi) + \varrho_3}\right)^2\right] \times e^{i\psi}. \tag{29}$$

Type VII

$\ell_2 = -4, \ell_3 = \frac{4(2\varrho_2 + \varrho_4)}{\varrho_1}, \ell_4 = -\frac{4\varrho_2^2 + 4\varrho_4\varrho_2 - \varrho_3^2}{\varrho_1^2}$, where $\varrho_1, \varrho_2, \varrho_3, \varrho_4$ are arbitrary constants.

$$\phi_9^{III}(x,t) = \left[\alpha_0 + \alpha_1\left(\frac{\varrho_1\sec^2(\xi)}{\varrho_2\tan(\xi) + \varrho_3 + \varrho_4\sec^2(\xi)}\right) + \alpha_2\left(\frac{\varrho_1\sec^2(\xi)}{\varrho_2\tan(\xi) + \varrho_3 + \varrho_4\sec^2(\xi)}\right)^2\right] \times e^{i\psi}. \tag{30}$$

Case IV

$\ell_1 = \ell_3 = 0$, Eq. (1) have solutions of the form $\phi_\eta^{IV}, (\eta = 1, 2, \ldots, 16)$.

Type I

$\ell_0 = \frac{1}{4}, \ell_2 = \frac{1-2m^2}{2}, \ell_4 = \frac{1}{4}$,

$$\Phi_3^{IV}(\xi) = \left(\alpha_0 + \alpha_1(cn\xi) + \alpha_2(cn\xi)^2\right) \times e^{i\psi}, \tag{31}$$

gives the bright optical soliton for $m \to 1$,

$$\Phi_3^{IV}(\xi) = \left(\alpha_0 + \alpha_1\operatorname{sech}(\xi) + \alpha_2(\operatorname{sech}(\xi))^2\right) \times e^{i\psi}, \tag{32}$$

and the periodic singular solutions for $m \to 0$,

$$\Phi_3^{IV}(\xi) = \left(\alpha_0 + \alpha_1\cos(\xi) + \alpha_2(\cos(\xi))^2\right) \times e^{i\psi}, \tag{33}$$

Type II

$\ell_0 = \frac{1}{4}, \ell_2 = \frac{1-2m^2}{2}, \ell_4 = \frac{1}{4}$,

$$\Phi_{13}^{IV}(\xi) = \left(\alpha_0 + \alpha_1(ns\xi \pm cs\xi) + \alpha_2(ns\xi \pm cs\xi)^2\right) \times e^{i\psi}, \tag{34}$$

gives the combined dark-singular wave solutions for $m \to 1$,

$$\Phi_{13}^{IV}(\xi) = \left(\alpha_0 + \alpha_1(\coth(\xi) + \operatorname{csch}(\xi)) + \alpha_2(\coth(\xi) + \operatorname{csch}(\xi))^2\right) \times e^{i\psi}, \tag{35}$$

and the periodic singular solutions for $m \to 0$,

$$\Phi_{13}^{IV}(\xi) = \left(\alpha_0 + \alpha_1(\cot(\xi) + \csc(\xi)) + \alpha_2(\cot(\xi) + \csc(\xi))^2\right) \times e^{i\psi}. \tag{36}$$

4. Discussion and results

To display a set of novel travelling wave solutions to the Eq. (1), Mathematica 11.0 is executed to demonstrate the behaviour of bit flow and to understand the complex structure of solitons for a set of limitations. The parameter $\alpha \in (0, 1]$ is the core constraint which simulate the flow rate propagation, plays a key rote in telecommunications and the theory of optical fibres.

Fig. 1 illustrates the solution $|\phi_1^I(x,t)|$ constructed in Case I (Type I) for $\kappa = -2, \omega = 0.1, \nu = 0.1, \alpha = 0.5, \sigma = 2, \varrho = 2, \theta = 2, \gamma = 1, \varsigma_1 = 1, \varsigma_2 = 2, \varsigma_3 = 3, \vartheta_1 = 5, \vartheta_2 = 1, \vartheta_3 = 2$, while Fig. 2 illustrates the solution $|\phi_3^I(x,t)|$ constructed in Case I (Type I) for $\kappa = -2, \omega = 0.1, \nu = -0.5, \alpha = 1, \sigma = 1, \varrho = 2, \theta = 2, \gamma = 1, \varsigma_1 = 1, \varsigma_2 = 2, \varsigma_3 = 3, \vartheta_1 = 3, \vartheta_2 = 1, \vartheta_3 = 1$, whereas Fig. 3 visualizes the solution $|\phi_{10}^I(x,t)|$ produced in Case I (Type I) for $\kappa = -2, \omega = 0.1, \nu = 0.1, \alpha = 0.5, \sigma = 2, \varrho = 2, \theta = 2, \gamma = 1, \varsigma_1 = 1, \varsigma_2 = 2, \varsigma_3 = 3, \vartheta_1 = 5, \vartheta_2 = 3, \vartheta_3 = 2$. Similarly, Fig. 4 illustrates the solution $|\phi_{11}^I(x,t)|$ constructed in Case I (Type I) for $\kappa = -2, \omega = 0.1, \nu = 0.1, \alpha = 0.5, \sigma = 2, \varrho = 2, \theta = 2, \gamma = 2, \varsigma_1 = 1, \varsigma_2 = 2, \varsigma_3 = 3, \vartheta_1 = 3, \vartheta_2 = 1, \vartheta_3 = -1$, while Fig. 5 visualizes the solution $|\phi_{17}^I(x,t)|$ constructed in Case I (Type II) for $\kappa = 0.1, \omega = 1, \nu = 0.1, \alpha = 1, \sigma = 2, \varrho = 2, \theta = 2, \gamma = 2, \varsigma_1 = 1, \varsigma_2 = 2, \varsigma_3 = 1, \vartheta_1 = 1, \vartheta_2 = 1, \vartheta_3 = 1$.

Comparably, Fig. 6 displays the solution $|\phi_1^{II}(x,t)|$ constructed in Case II (Type I) for $\kappa = -2, \omega = 0.1, \nu = 0.1, \alpha = 0.5, \sigma = 2, \varrho = 2, \theta = 2, \gamma = 2, \varsigma_1 = 1, \varsigma_2 = 2, \varsigma_3 = 3, \vartheta_1 = 0, \vartheta_2 = -1, \vartheta_3 = 1$ whereas Fig. 7 reveals the solution $|\phi_1^{III}(x,t)|$ constructed in Case III (Type I) for $\kappa = -2, \omega = 0.1, \nu = 0.1, \alpha = 0.5, \sigma = 2, \varrho = 2, \theta = 2, \gamma = 2, \varsigma_1 = 5, \varsigma_2 = 2, \varsigma_3 = 3, \varrho_1 = 1, \varrho_2 = 2, \varrho_3 = 3$ and Fig. 8 displays the solution $|\phi_3^{III}(x,t)|$ constructed in Case III (Type I) for $\kappa = 1, \omega = 0.5, \nu = 0.1, \alpha = 1, \sigma = 2, \varrho = 2, \theta = 2, \gamma = 2, \varsigma_1 = 1, \varsigma_2 = 2, \varsigma_3 = 3, \varrho_1 = 1, \varrho_2 = 2, \varrho_3 = 3$.

Likewise, Fig. 9 illustrates the solution $|\phi_1^{IV}(x,t)|$ constructed in Case IV ($m \to 1$) for $\kappa = -2, \omega = 0.1, \nu = 0.1, \alpha = 0.5, \sigma = 2, \varrho = 2, \theta = 2, \gamma = 1, \varsigma_1 = 1, \varsigma_2 = 2, \varsigma_3 = 3$, while Fig. 10 represents the solution $|\phi_1^{IV}(x,t)|$ constructed in Case IV ($m \to 0$) for $\kappa = -2, \omega = 0.1, \nu = 0.1, \alpha = 0.5, \sigma = 2, \varrho = 2, \theta = 2, \gamma = 1, \varsigma_1 = 1, \varsigma_2 = 2, \varsigma_3 = 3$.

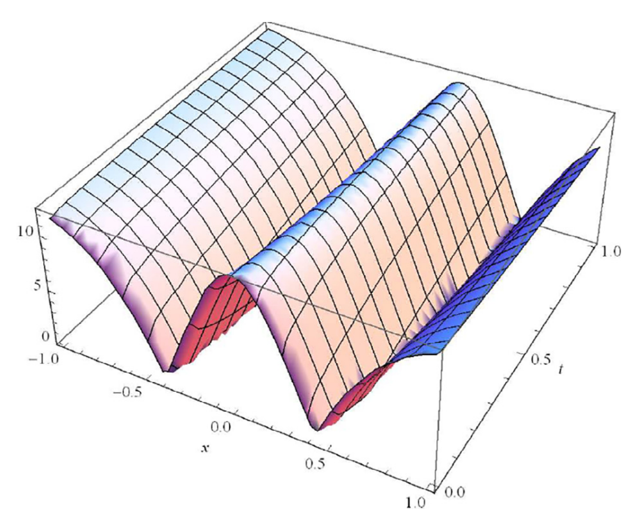

Fig. 1. $|\Phi_1^I(x,t)|$: $\kappa = -2, \omega = 0.1, \nu = 0.1, \alpha = 0.5, \sigma = 2, \varrho = 2, \theta = 2, \gamma = 1, \varsigma_1 = 1, \varsigma_2 = 2, \varsigma_3 = 3, \vartheta_1 = 5, \vartheta_2 = 1, \vartheta_3 = 2$.

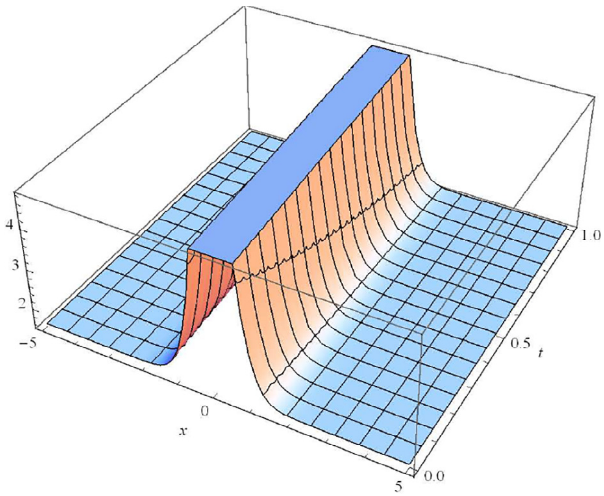

Fig. 2. $|\Phi_3^I(x,t)|$: $\kappa = -2$, $\omega = 0.1$, $v = -0.5$, $\alpha = 1$, $\sigma = 1$, $\varrho = 2$, $\theta = 2$, $\gamma = 1$, $\varsigma_1 = 1$, $\varsigma_2 = 2$, $\varsigma_3 = 3$, $\vartheta_1 = 3$, $\vartheta_2 = 1$, $\vartheta_3 = 1$.

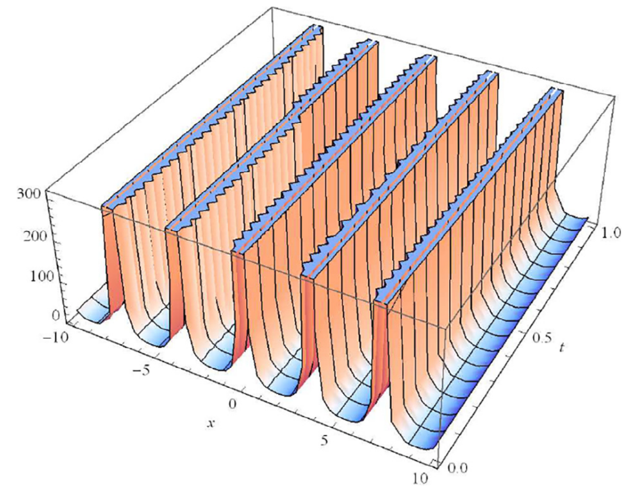

Fig. 5. $|\Phi_{17}^I(x,t)|$: $\kappa = 0.1$, $\omega = 1$, $v = 0.1$, $\alpha = 1$, $\sigma = 2$, $\varrho = 2$, $\theta = 2$, $\gamma = 2$, $\varsigma_1 = 1$, $\varsigma_2 = 2$, $\varsigma_3 = 1$, $\vartheta_1 = 1$, $\vartheta_2 = 1$, $\vartheta_3 = 1$.

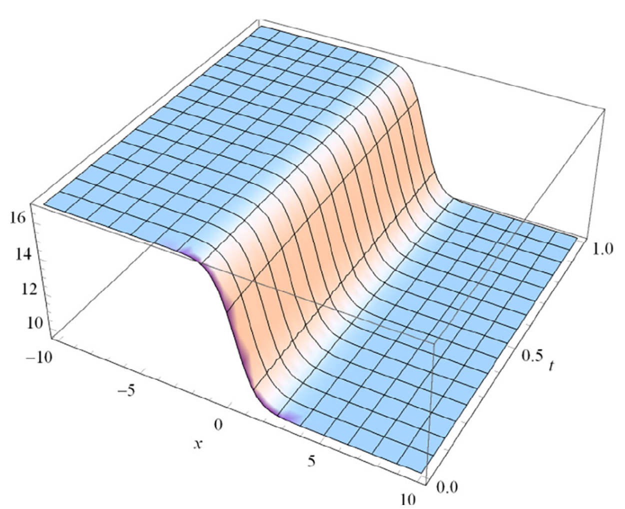

Fig. 3. $|\Phi_{10}^I(x,t)|$: $\kappa = -2$, $\omega = 0.1$, $v = 0.1$, $\alpha = 0.5$, $\sigma = 2$, $\varrho = 2$, $\theta = 2$, $\gamma = 1$, $\varsigma_1 = 1$, $\varsigma_2 = 2$, $\varsigma_3 = 3$, $\vartheta_1 = 5$, $\vartheta_2 = 3$, $\vartheta_3 = 2$.

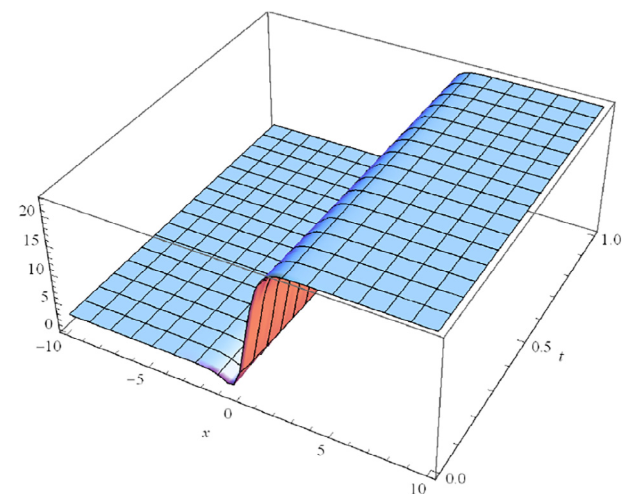

Fig. 6. $|\Phi_1^{II}(x,t)|$: $\kappa = -2$, $\omega = 0.1$, $v = 0.1$, $\alpha = 0.5$, $\sigma = 2$, $\varrho = 2$, $\theta = 2$, $\gamma = 2$, $\varsigma_1 = 1$, $\varsigma_2 = 2$, $\varsigma_3 = 3$, $\vartheta_1 = 0$, $\vartheta_2 = -1$, $\vartheta_3 = 1$.

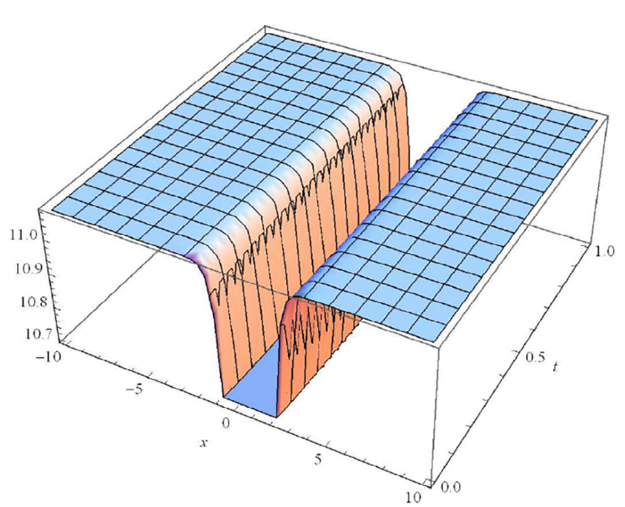

Fig. 4. $|\Phi_{11}^I(x,t)|$: $\kappa = -2$, $\omega = 0.1$, $v = 0.1$, $\alpha = 0.5$, $\sigma = 2$, $\varrho = 2$, $\theta = 2$, $\gamma = 2$, $\varsigma_1 = 1$, $\varsigma_2 = 2$, $\varsigma_3 = 3$, $\vartheta_1 = 3$, $\vartheta_2 = 1$, $\vartheta_3 = -1$.

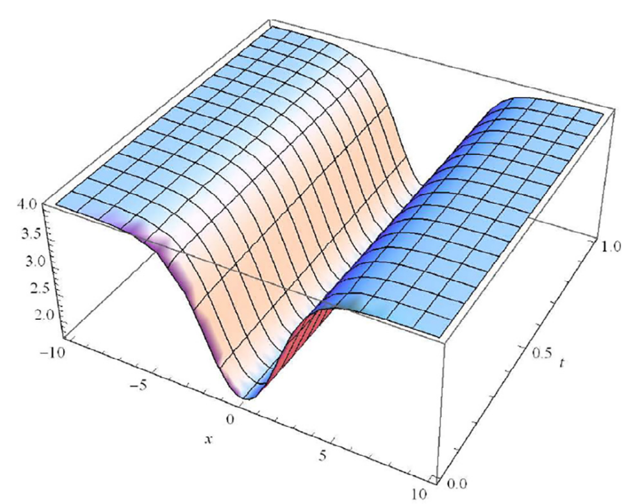

Fig. 7. $|\Phi_1^{III}(x,t)|$: $\kappa = -2$, $\omega = 0.1$, $v = 0.1$, $\alpha = 0.5$, $\sigma = 2$, $\varrho = 2$, $\theta = 2$, $\gamma = 2$, $\varsigma_1 = 5$, $\varsigma_2 = 2$, $\varsigma_3 = 3$, $\varrho_1 = 1$, $\varrho_2 = 2$, $\varrho_3 = 3$.

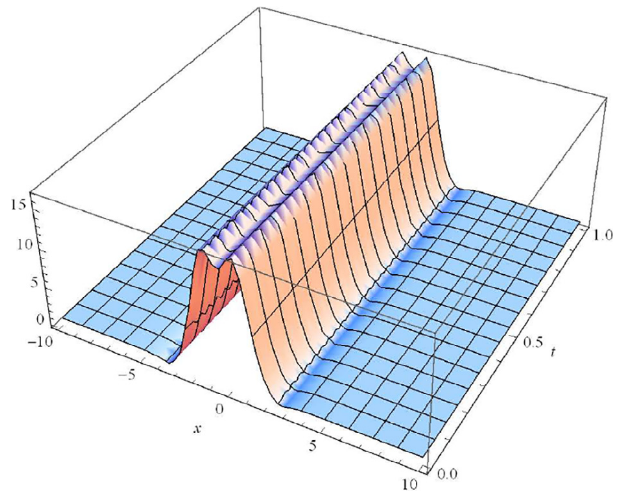

Fig. 8. $|\Phi_3^{III}(x,t)|$: $\kappa = 1$, $\omega = 0.5$, $\nu = 0.1$, $\alpha = 1$, $\sigma = 2$, $\varrho = 2$, $\theta = 2$, $\gamma = 2$, $\varsigma_1 = 1$, $\varsigma_2 = 2$, $\varsigma_3 = 3$, $\varrho_1 = 1$, $\varrho_2 = 2$, $\varrho_3 = 3$.

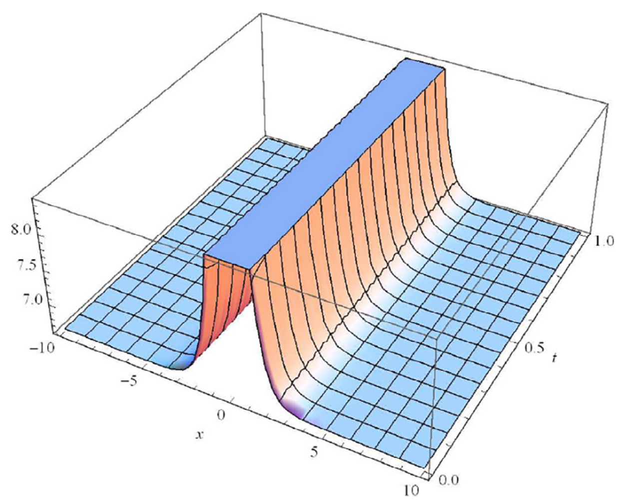

Fig. 9. $|\Phi_1^{IV}(x,t)|$ $m \to 1$: $\kappa = -2$, $\omega = 0.1$, $\nu = 0.1$, $\alpha = 0.5$, $\sigma = 2$, $\varrho = 2$, $\theta = 2$, $\gamma = 1$, $\varsigma_1 = 1$, $\varsigma_2 = 2$, $\varsigma_3 = 3$.

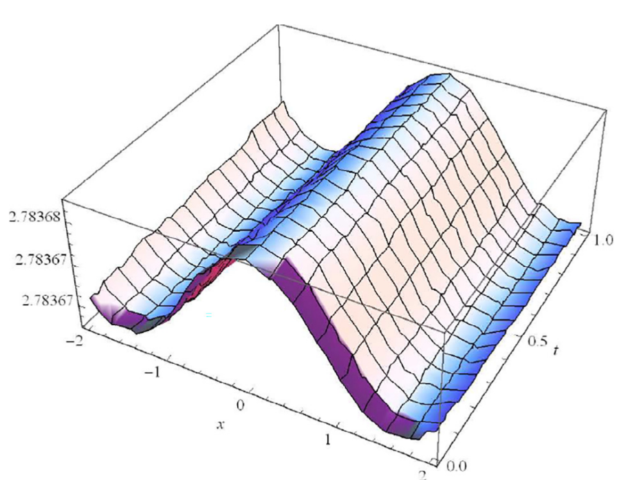

Fig. 10. $|\Phi_1^{IV}(x,t)|$ $m \to 0$: $\kappa = -2$, $\omega = 0.1$, $\nu = 0.1$, $\alpha = 0.5$, $\sigma = 2$, $\varrho = 2$, $\theta = 2$, $\gamma = 1$, $\varsigma_1 = 1$, $\varsigma_2 = 2$, $\varsigma_3 = 3$.

5. Conclusion

In this paper, the resonant fractional nonlinear Schrödinger equation with quadratic-cubic nonlinearity is investigated with the help of the conformable derivative associated to the extended FAN sub-equation method. The latest scientific computing tools *Mathematica*11.0 is implemented to visualize the dynamics of the complex fractional model (1). The structure of the model is displayed for various set of parameters in an intensive way. To further analyze the behavior of the nonlinear fractional phenomenon, a number of significant solitons have been systematically identified, including bright, dark, singular, combination, optical, singular optical, and gloss-singular combination solitons, as shown in Figs. 1–10. The parameter α is the core constraint which simulate the flow rate propagation, plays a key rote in telecommunications and the theory of optical fibres. The computational results are very encouraging, powerful, efficient and can also be extended to have advanced exact solutions for many complex models from different branches of engineering and applied sciences.

Availability of supporting data

Not applicable.

Funding

This work was supported by the National Natural Science Foundation of China (Grant Nos. 11971142, 11871202, 61673169, 11701176, 11626101, 11601485).

6. Author's contributions

All authors contributed equally to the writing of this paper. All authors read and approved the final manuscript.

Declaration of Competing Interest

The authors declare that they have no known competing financial interests or personal relationships that could have appeared to influence the work reported in this paper.

Acknowledgements

The authors would like to express their sincere thanks to the support of National Natural Science Foundation of China.

References

Baskonus, H.M., Sulaiman, T.A., Bulut, H., Aktürk, T., 2018. Investigations of dark, bright, combined dark-bright optical and other soliton solutions in the complex cubic nonlinear Scrödinger equation with d-potential. Superlatt. Microstruct. 115, 19–29.

Bhrawy, A., Alshaery, A., Hilal, E., Khan, K.R., Mahmood, M.F., Biswas, A., 2014. Optical soliton perturbation with spatio-temporal dispersion in parabolic and dual-power law media by semi-inverse variational principle. Optik 125 (17), 4945–4950.

El-Wakil, S.A., Abdou, M.A., 2008. The extended Fan sub-equation method and its applications for a class of nonlinear evolution equations. Chaos Solitons Fract. 36 (2), 343–353.

Eslami, M., Mirzazadeh, M., Biswas, A., 2013. Soliton solutions of the resonant nonlinear Schrödinger's equation in optical fibers with time dependent coefficients by simplest equation approach. J. Mod. Opt. 60 (19), 1627–1636.

Ghanbari, B., Inc, M., Rada, L., 2019a. Solitary wave solutions to the Tzitzeica type equations obtained by a new efficient approach. J. Appl. Anal. Comput. 9 (2), 568–589.

Ghanbari, B., Yusuf, A., Baleanu, D., 2019b. The new exact solitary wave solutions and stability analysis for the (2+1)-dimensional Zakharov-Kuznetsov equation. Adv. Differ. Equ. 2019 (1), 1–15.

Ghanbari, B., Nisar, K.S., Aldhaifallah, M., 2020. Abundant solitary wave solutions to an extended nonlinear Schrödinger's equation with conformable derivative using an efficient integration method. Adv. Differ. Equ. 2020 (1), 1–25.
Goswami, A., Singh, J., Kumar, D., 2020. Numerical computation of fractional Kersten-Krasil-shchik coupled KdV-mKdV system occurring in multi-component plasmas. AIMS Math. 5 (3), 2346.
Hashemi, M.S., Inc, M., Bayram, M., 2019. Symmetry properties and exact solutions of the time fractional Kolmogorov-Petrovskii-Piskunov equation. Rev. Mex. de Fis. 65 (5), 529–535.
Hong, B., Lu, D., 2009. New Jacobi elliptic functions solutions for the higher-order nonlinear Scrödinger equation. Int. J. Nonlinear Sci. 7 (3), 360–367.
Hosseini, K., Mirzazadeh, M., Gomez-Aguilar, J.F., 2020a. Soliton solutions of the Sasa-Satsuma equation in the monomode optical fibers including the beta-derivatives. Optik 224, 165425.
Hosseini, K., Mirzazadeh, M., Vahidi, J., Asghari, R., 2020b. Optical wave structures to the Fokas-Lenells equation. Optik 207, 164450.
Hosseini, K., Korkmaz, A., Bekir, A., Samadani, F., Zabihi, A., Topsakal, M., 2020c. New wave form solutions of nonlinear conformable time-fractional Zoomeron equation in (2+1)-dimensions. Waves Random Complex Media, 1–11.
Kalim, U.T., Younis, M., Rizvi, S.T.R., 2018. Optical solitons in monomode fibers with higher order nonlinear Schrödinger equation. Optik 154, 360–371.
Korpinar, Z., Inc, M., Bayram, M., Hashemi, M.S., 2019. New optical solitons for Biswas-Arshed equation with higher order dispersions and full nonlinearity. Optik 206, 163332.
Liu, J.G., Osman, M.S., Wazwaz, A.M., 2019. A variety of nonautonomous complex wave solutions for the (2+ 1)-dimensional nonlinear Schrödinger equation with variable coefficients in nonlinear optical fibers. Optik. 180, 917–923.
Mahak, N., Akram, G., 2019. Exact solitary wave solutions by extended rational sine-cosine and extended rational sinh-cosh techniques. Phys. Scr. 94, (11) 115212.
Manafian, J., Lakestani, M., 2017. A new analytical approach to solve some of the fractional-order partial differential equations. Indian J. Phys. 91, 243–258.
Mehdinejadiani, B., Parviz, F., 2020. Analytical solutions of space fractional Boussinesq equation to simulate water table profiles between two parallel drainpipes under different initial conditions. Agric. Water Manag. 240, 106324.
Miller, K.S., Ross, B., 1993. An Introduction to the Fractional Calculus and Fractional Differential Equations. Wiley-Interscience Publication, Wiley, New York.
Munusamy, K., Ravichandran, C., Nisar, K.S., Ghanbari, B., 2020. Existence of solutions for some functional integrodifferential equations with nonlocal conditions. Math. Methods Appl. Sci. 43(17) 30, 10319–10331.
Rezazadeh, H., 2018. New solitons solutions of the complex Ginzburg-Landau equation with Kerr law nonlinearity. Optik 167, 218–227.
Seadawy, A.R., Lu, D., 2017. Bright and dark solitary wave soliton solutions for the generalized higher order nonlinear Schrödinger equation and its stability. Results Phys. 7, 43–48.
Seadawy, A.R., Iqbal, M., Lu, D., 2020. Propagation of kink and anti-kink wave solitons for the nonlinear damped modified Korteweg-de Vries equation arising in ion-acoustic wave in an unmagnetized collisional dusty plasma. Physica A Stat. Mech. Appl. 544, 123560.
Singh, J., Ahmadian, A., Rathore, S., Kumar, D., Baleanu, D., Salimi, M., Salahshour, S., 2021a. An efficient computational approach for local fractional Poisson equation in fractal media. Numer. Methods Partial Differ. 37 (2), 1439–1448.
Singh, J., Kumar, D., Purohit, S.D., Mishra, A.M., Bohra, M., 2021b. An efficient numerical approach for fractional multidimensional diffusion equations with exponential memory. Numer. Methods Partial Differ. 37 (2), 1631–1651.
Singh, Y., Gill, V., Singh, J., Kumar, D., Khan, I., 2021c. Computable generalization of fractional kinetic equation with special functions. J. King Saud Univ. Sci. 33, (1) 101221.
Triki, H., Biswas, A., Moshokoa, S.P., Belic, M., 2017. Optical solitons and conservation laws with quadratic-cubic nonlinearity. Optik 128, 63–70.
Wazwaz, A.M., 2006. Explicit and implicit solutions for the one-dimensional cubic and quintic complex Ginzburg-Landau equations. Appl. Math. Lett. 19 (10), 1007–1012.
Younis, M., Cheemaa, N., Mehmood, S.A., Rizvi, S.T.R., Bekir, A., 2020. A variety of exact solutions to (2+1)-dimensional schrödinger equation. Waves Random Complex Media 30, 490–499.
Zhang, X., Chen, Y., 2019. Inverse scattering transformation for generalized nonlinear Schrödinger equation. Appl. Math. Lett. 98, 306–313.